THE EXTENSION OF DISCRETE-TIME FLUTTER MARGIN

Hiroshi Torii
Meijo University
htorii@meijo-u.ac.jp

Keywords: *aeroelasticity, flutter prediction, flutter test, ARMA model, flutter margin*

Abstract

The extension of the discrete-time flutter margin introduced in the previous work is proposed. For the three-mode system, the effectiveness of the proposed method is shown from the analysis and the numerical simulation using a two-dimensional wing model, and also the application to the wind tunnel flutter test data.

1 Introduction

Since flutter is the self excited vibration which causes a fatal damage to an airfoil, we have to pay utmost attention to the occurrence of flutter in the airplane design and development. At the final stage of development, therefore, we has to conduct the flutter tests to check that flutter does not occur in the flight envelop, and to evaluate the flutter boundary. Since the flutter tests are carried out only in the safety range far below the critical point to avoid structural damage during the tests, the flutter boundary is predicted from the behavior of some stability measure plotted against the flight speed or the dynamic pressure. The stability margin from the flutter boundary has been conventionally evaluated by the modal damping. For a reliable prediction of flutter, it is quite significant to measure the modal damping accurately from the flight test data. However an accurate evaluation of damping of a wing in an airstream is not necessarily an easy task, so that lots of works on the flutter prediction have been directed to improve the accuracy or efficiency of damping estimation. It is pointed out, however, that the damping is not always an appropriate parameter to predict the flutter boundary [1], that is, for a so-called explosive type of flutter it gives no sign of instability up to the neighborhood of the critical speed.

As an alternative approach, several researchers have attempted to propose more suitable parameters for the flutter prediction than the modal damping. Among them, the flutter margin introduced by Zimmermann and Weissenburger [1] is the most famous and successful one. The flutter margin decreases almost monotonically toward zero as the dynamic pressure increases, which is a very suitable property for the flutter prediction, though it is applicable only to binary-flutter. The extension to a three-mode system is attempted by Price and Lee [2].

Since the flutter margin is defined based on the continuous-time system, it is not convenient for digital processing. In the discrete-time domain, Matsuzaki and Ando [3] have proposed to use Jury's stability parameter as the indicator of stability margin, which is the stability criterion for the discrete-time system and are calculated from the Autoregressive Moving Average (ARMA) model identified. Then authors [4] modified Jury's parameters and introduced the new parameter called the flutter margin for the discrete-time system (FMDS), which is approximately equivalent to the flutter margin introduced in Ref.1. Though the FMDS has superior properties as the flutter prediction parameter, it is applicable to the data which include only two coupling modes. This should be relaxed to apply this method to the actual flutter test data. Though the extension of the FMDS to the multimode system was attempted [5], a mathematical foundation or a theoretical consideration of the parameter introduced was not clear, and the parameter is not consistent with the FMDS for the two-mode system as

mentioned by McNamara and Friedmann [6]. Therefore the extension of the FMDS is still an open problem.

The purpose of this work is to extend the FMDS to the three-mode system. A new flutter prediction parameter is proposed based on Jury's stability determinant method. The properties of the parameter are investigated using a two-dimensional wing model. Then we show the application results to the wind tunnel flutter test data which are measured under the stationary and non-stationary conditions.

2 Flutter Margin Method

From the modal damping and frequency, we can obtain the characteristic roots of the j-th mode.

$$s_j = \alpha_j + i\beta_j, \quad s_j^* = \alpha_j - i\beta_j$$

The characteristic equation corresponding to the coupling mode, s_1 and s_2, which causes flutter is expressed by

$$(s-s_1)(s-s_1^*)(s-s_2)(s-s_2^*)=0$$

that is,

$$s^4 + P_3 s^3 + P_2 s^2 + P_1 s + P_0 = 0 \qquad (1)$$

Based on Routh's stability criteria to Eq.(1), Zimmermann defined the flutter margin:

$$F = -\left(\frac{P_1}{P_3}\right)^2 + P_2\left(\frac{P_1}{P_3}\right) - P_0 \qquad (2)$$

The value of F indicates the stability margin, that is, F is positive in the subcritical speed range and becomes zero at the flutter boundary. Equation (2) is also expressed as

$$F = \left\{\left(\frac{\beta_2^2-\beta_1^2}{2}\right)+\left(\frac{\alpha_2^2-\alpha_1^2}{2}\right)\right\}^2$$
$$+4\alpha_1\alpha_2\left\{\left(\frac{\beta_2^2+\beta_1^2}{2}\right)+2\left(\frac{\alpha_2^2+\alpha_1^2}{2}\right)^2\right\}$$
$$-\left\{\left(\frac{\alpha_2-\alpha_1}{\alpha_2+\alpha_1}\right)\left(\frac{\beta_2^2-\beta_1^2}{2}\right)+2\left(\frac{\alpha_2^2+\alpha_1^2}{2}\right)^2\right\}^2$$

This is a convenient expression to evaluate the value of F from the aeroelastic characteristics estimated at an experiment.

Moreover, from the analysis using a two-dimensional wing model, the flutter margin is shown to be a quadratic function of the dynamic pressure.

3 Discrete-Time Flutter Margin Method

Unlike the flutter margin, the FMDS introduced in Ref.4 is defined based on the time-series model, so that it is suitable for the digital data processing, and it doesn't need the modal damping and frequency.

After preprocessed through the band-pass filter so as to include only the coupling mode, sampled data is identified by the ARMA model

$$y_t + \alpha_1 y_{t-1} + \alpha_2 y_{t-2} + \alpha_3 y_{t-3} + \alpha_4 y_{t-4}$$
$$= e_t + \beta_1 e_{t-1} + \beta_2 e_{t-2} + \beta_{t-m} e_{t-m} \qquad (3)$$

where y_t is the data observed at time t, and e_t a white noise. The order, m, in the right hand side of Eq.(3) is determined by the Akaike Information Criteria (AIC). The left hand side corresponds to the characteristic equation of the system:

$$G(z) = z^4 + \alpha_1 z^3 + \alpha_2 z^2 + \alpha_3 z + \alpha_4$$
$$= \prod_{i=1}^{2}(z-z_i)(z-z_i^*)$$

where z_i is the characteristic root.

The stability margin of the system is measured by

$$F_z = \frac{\det(X_3 - Y_3)}{(1-\alpha_4)^2} \qquad (4)$$

where

$$X_3 = \begin{pmatrix} 1 & \alpha_1 & \alpha_2 \\ 0 & 1 & \alpha_1 \\ 0 & 0 & 1 \end{pmatrix}, \quad Y_3 = \begin{pmatrix} \alpha_2 & \alpha_3 & \alpha_4 \\ \alpha_3 & \alpha_4 & 0 \\ \alpha_4 & 0 & 0 \end{pmatrix}$$

and $\alpha_1 \sim \alpha_4$ are the coefficients of Eq.(3).

The analysis using a two-dimensional wing model shows that Eqs.(2) and (4) have approximately the relation

$$F_z \approx T^4 F = T^4\left[C_2\left(C_{L_\alpha} q\right)^2 + C_1\left(C_{L_\alpha} q\right) + C_0\right]$$

where T is a sampling interval and q is the dynamic pressure. Therefore the parameter F_z has a similar property to the flutter margin, that is, the value of F_z decreases monotonically and almost linearly toward zero in the subcritical range with the increase of the dynamic pressure.

4 Extension of FMDS

Though the FMDS has a superior property for the flutter prediction, it is applicable only to the two-mode system. Here we attempt to extend it to the three-mode system. For the data having three modes is identified by the following ARMA model instead of Eq.(3).

$$\begin{aligned} & y_t + \alpha_1 y_{t-1} + \alpha_2 y_{t-2} + \cdots + \alpha_6 y_{t-6} \\ & \quad = e_t + \beta_1 e_{t-1} + \cdots + \beta_{t-m} e_{t-m} \end{aligned} \tag{5}$$

Therefore, we obtain the characteristic equation

$$\begin{aligned} G(z) &= z^6 + \alpha_1 z^5 + \cdots + \alpha_5 z + \alpha_6 \\ &= \prod_{i=1}^{3} (z - z_i)(z - z_i^*) \end{aligned} \tag{6}$$

Here we propose a new flutter prediction parameter

$$F_z^{(3)} = \frac{\det\left(X_5 - Y_5\right)}{\left(1-\alpha_6\right)^3} \tag{7}$$

where X_5 and Y_5 are matrices whose elements consists of the coefficients of Eq.(5) as follows.

$$X_5 = \begin{pmatrix} 1 & \alpha_1 & \alpha_2 & \alpha_3 & \alpha_4 \\ 0 & 1 & \alpha_1 & \alpha_2 & \alpha_3 \\ 0 & 0 & 1 & \alpha_1 & \alpha_2 \\ 0 & 0 & 0 & 1 & \alpha_1 \\ 0 & 0 & 0 & 0 & 1 \end{pmatrix}, \quad Y_5 = \begin{pmatrix} \alpha_2 & \alpha_3 & \alpha_4 & \alpha_5 & \alpha_6 \\ \alpha_3 & \alpha_4 & \alpha_5 & \alpha_6 & 0 \\ \alpha_4 & \alpha_5 & \alpha_6 & 0 & 0 \\ \alpha_5 & \alpha_6 & 0 & 0 & 0 \\ \alpha_6 & 0 & 0 & 0 & 0 \end{pmatrix}$$

We can express the equation in the denominator of Eq.(7) using the characteristic roots z_i as

$$1-\alpha_6 = 1 - |z_1|^2 |z_2|^2 |z_3|^2$$

If the system is stable, all roots have the absolute value less than 1, so that the above equation has a positive value at and below the critical speed. The numerator of Eq.(6) is expressed as

$$\begin{aligned} \det\left(X_5 - Y_5\right) &= \prod_{1 \le i < j \le 6} (1 - z_i z_j) \\ &= \left(1 - z_1^2\right)\left(1 - z_2^2\right)\left(1 - z_3^2\right) \\ &\times \left|1 - z_1 z_2\right|^2 \left|1 - z_1 z_3\right|^2 \left|1 - z_2 z_3\right|^2 \\ &\times \left|1 - z_1 z_2^*\right|^2 \left|1 - z_1 z_3^*\right|^2 \left|1 - z_2 z_3^*\right|^2 \end{aligned}$$

where $z_4=z_1^*$, $z_5=z_2^*$ and $z_6=z_3^*$. Therefore, it is positive as long as all roots locate in a unit circle, and becomes zero when one of the roots reaches a unit circle. This means in the flutter prediction that the parameter $F_z^{(3)}$ is positive in the subcritical range and becomes zero at the speed of flutter onset.

5 Analysis and Simulation using Two-Dimensional Wing Model

To study the property of $F_z^{(3)}$, we carry out the analysis using a three-degree-of-freedom wing model illustrated in Fig. 1. The values used in this model are a = -0.4, c = 0.6, $\mu = m/(\pi\rho b^2)$ = 40, $S_\alpha/(mb)$ = 0.2, $S_\beta/(mb)$ = 0.0125, $I_\alpha/(mb^2)$ = 0.25, $I_\beta/(mb^2)$ = 0.00625, $\omega_h = \sqrt{K_h/m} = 50$, $\omega_\alpha = \sqrt{K_\alpha/I_\alpha} = 100$ and $\omega_\beta = \sqrt{K_\beta/I_\beta} = 200$.

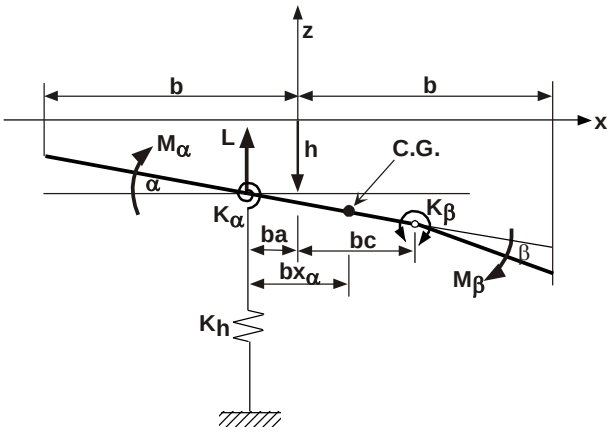

Fig. 1 Two-dimensional wing model

From equations of motion of the wing, we can obtain the characteristic roots and, therefore, the parameter $F_z^{(3)}$ using Eqs.(6) and (7). Figure 2 depicts the behavior of $F_z^{(3)}$ plotted against the dynamic pressure normalized by the flutter

boundary q_F. The modal frequency and damping are also obtained from the characteristic roots, and depicted in Fig.3 and Fig.4, respectively.

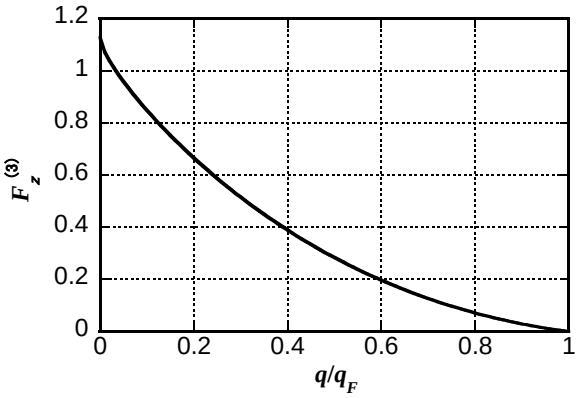

Fig.2 Behavior of $F_z^{(3)}$

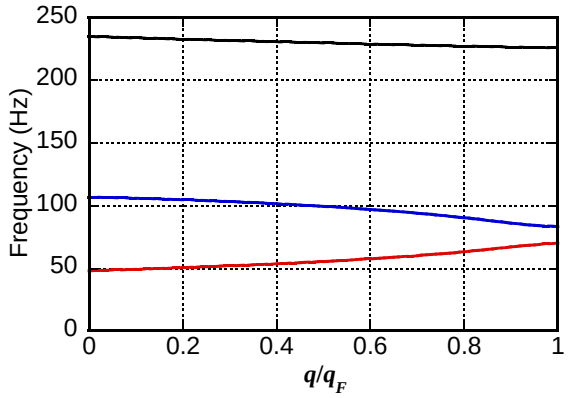

Fig.3 Behavior of the modal frequency

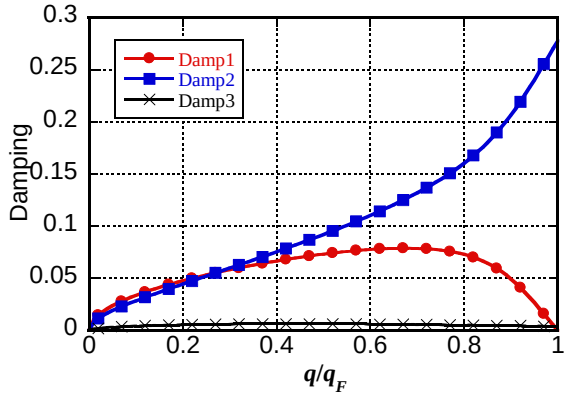

Fig.4 Behavior of the modal damping

As shown in Fig.3 and Fig.4, the first and the second modes are coupling, and the first mode becomes unstable. Figure 2 shows that the parameter $F_z^{(3)}$ decreases monotonically in the whole subcritical range as the dynamic pressure increases, whereas the critical mode damping starts to decrease around 80% of q_F as shown in Fig.4. Therefore if we use $F_z^{(3)}$ as the flutter prediction parameter, we can make an accurate and reliable prediction of flutter in comparison with the modal damping method.

To examine the robustness of the property of $F_z^{(3)}$, the value of ω_β is changed to 170, and the other configuration remains at the same value. The values of $F_z^{(3)}$, the modal frequency and the modal damping are shown in Fig.5 to Fig.7, respectively. As shown in Fig.7 the third mode is critical and the type of flutter is mild for this model, whereas the property of $F_z^{(3)}$, decreasing monotonically in the whole subcritical range, is conserved.

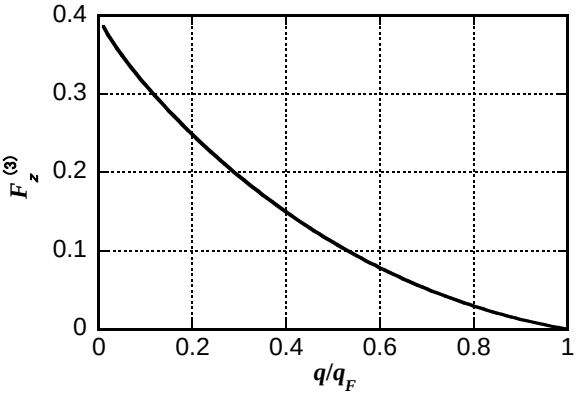

Fig.5 Behavior of $F_z^{(3)}$ for the second model

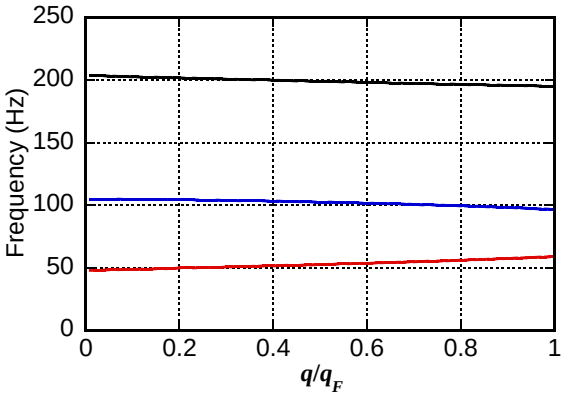

Fig.6 Behavior of the modal frequency for the second model

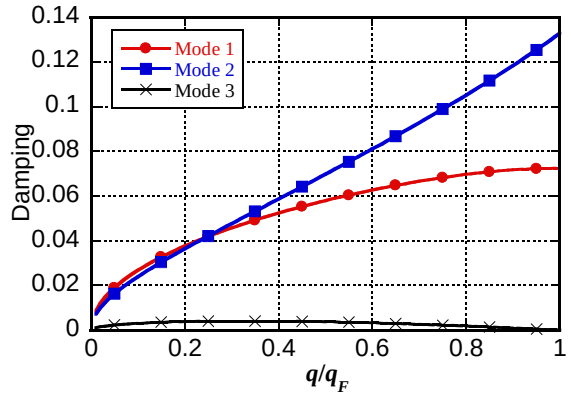

Fig.7 Behavior of the modal damping for the second model

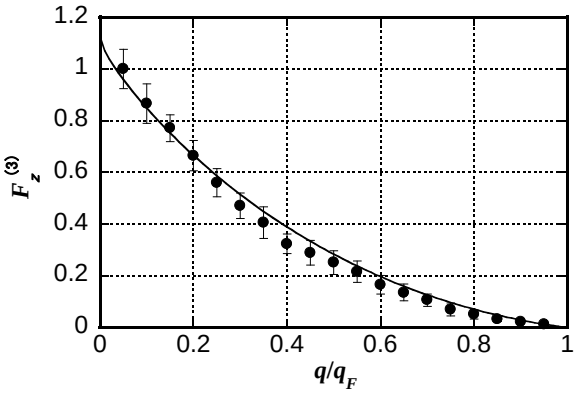

Fig.8 Average and standard deviation of $F_z^{(3)}$

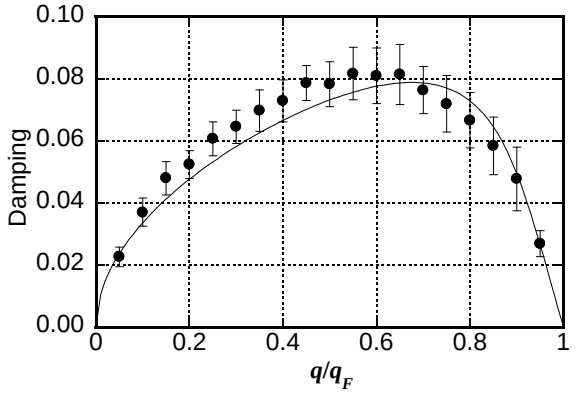

Fig.9 Average and standard deviation of the modal damping

Also the numerical simulation is conducted for the first model. Random response data is generated by a white noise input to equations of motion. The sampling interval is T=0.01 sec. The number of data used to estimate the ARMA model is 6000. The estimation is carried out 50 times at each dynamic pressure. The average and its standard deviation for estimated $F_z^{(3)}$ and the modal damping are depicted in Fig.8 and Fig.9, in which symbols show the average and an error bar indicates the standard deviation. The solid lines show the true value given in Fig.2 and Fig.4.

Figure 8 shows that most estimates of $F_z^{(3)}$ are located near the true value with a small deviation. This is an important property for the accurate and reliable identification of flutter. Meanwhile, estimated damping of the first mode, which is the critical mode, is slightly higher than the true value in the range of $q/q_F < 0.7$ and lower in the other range, and its standard deviation is a little bigger than that of $F_z^{(3)}$.

6 Application to Flutter Test Data

To check the feasibility of this method in an actual situation, we apply it to the data measured in wind tunnel flutter tests. Figure 10 illustrates the planform of a wing model, which is made of aluminum alloy flat plate of 2 mm thickness, and has a double-wedge at the leading and trailing edges. The modal frequencies obtained by the FEM analysis and the vibration test are summarized in Table 1.

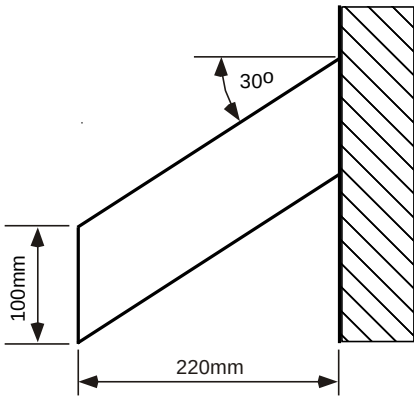

Fig.10 Planform of wing model

Table 1 Modal frequency of wing model (Hz)

Mode No.	FEM	Experiment
1	27.9	27.2
2	145.7	142.0
3	207.1	192.3

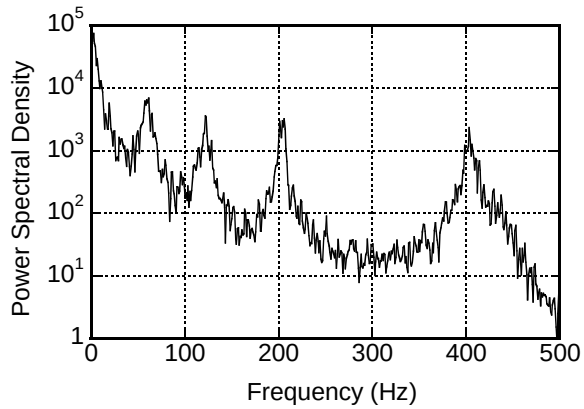

Fig.11 Power spectral density of data at q=75.5

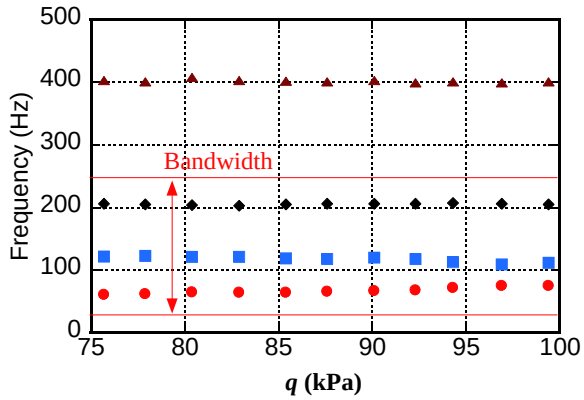

Fig.12 Modal frequencies

The Random response of the wing to a flow turbulence is measured by the strain gauge attached on the surface, and is sampled at a sampling interval T=2 msec. The bandwidth of the data is limited by passing through a filter so as to include only the lowest three modes. Figure 11 gives the power spectral density of the data measured at q=75.5 kPa, and the modal frequency of the lowest 4 modes is plotted in Fig.12. From these figures, we set the bandwidth of a filter between 30 Hz and 250 Hz to cut a low frequency noise and higher modes. The observed flutter boundary in the experiment is q_F=113.5 kPa, where flutter occurs by a coupling of the first and the second modes, and the second mode becomes unstable.

Wind tunnel tests are conducted (i) under the stationary condition in which the data are measured at 11 points of dynamic pressure from q = 75.7 to 99.4 kPa and the dynamic pressure is fixed during each test, and (ii) under the non-stationary condition in which the dynamic pressure is swept from q = 76.0 to 116.6 kPa at a rate of 2.6 kPa/sec. The Mach number is M = 2.51 for all tests.

(i) Results of stationary tests

The estimated value of $F_z^{(3)}$ are plotted against the dynamic pressure in Fig.13. The number of data used for an estimation is 6000, which corresponds to the measurement of 12 sec. These values decrease almost linearly as the increase of the dynamic pressure. Therefore a linear fitting drawn by a solid straight line gives a good prediction of q_F. The point of flutter onset observed in the experiment is expressed by a red symbol 'x'. In this case, the flutter boundary predicted by the extrapolation of the regression line is $\hat{q}_F$ =114.3 kPa, so it is 0.7% higher than the actual value. The goodness of fit for this regression line is R^2=0.986. This means that the linear fitting is reasonable to these data.

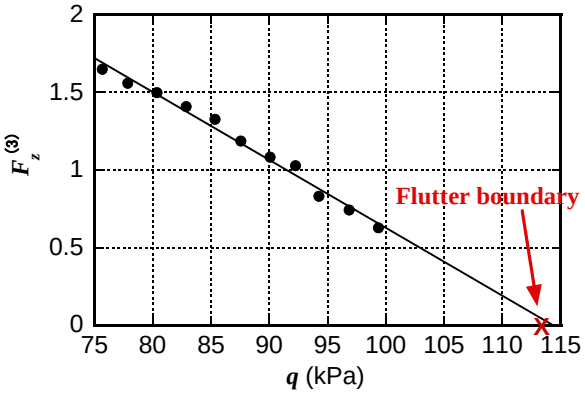

Fig.13 Estimated $F_z^{(3)}$ and the flutter prediction

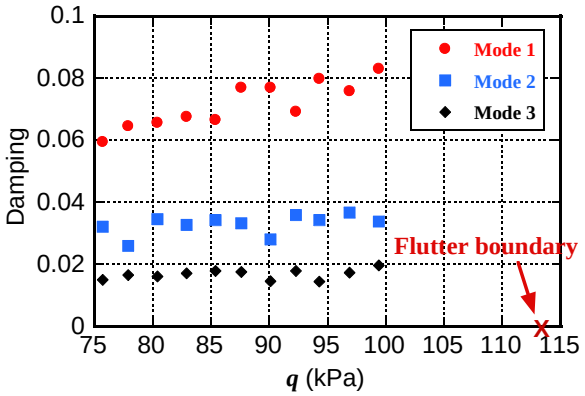

Fig.14 Estimated modal damping

In Fig.14 the estimated values of modal damping are depicted. The first mode has a little upward trend, and the other two modes show no trend in evidence from the tests in this range. Therefore, it is impossible to predict the flutter boundary, the point shown by 'x', based on these estimated values. We need to conduct the tests at higher dynamic pressure than this to predict the flutter boundary based on the modal damping.

(ii) Results of non-stationary test

For non-stationary data, we use a recursive identification procedure to estimate the parameters in real time, in which the coefficients of the ARMA model are updated at every sampling instance, and the value of $F_z^{(3)}$ and the modal damping is also renewed. The estimation result of $F_z^{(3)}$ is given in Fig.15, where red circles are the values estimated in the stationary tests. Base on these values we evaluate the accuracy of estimation. This figure shows that the real-time estimation gives the similar value as the stationary case, and decreases almost linearly toward zero.

The real-time estimation of modal damping, however, gives quite different values from the results of the stationary tests as shown in Fig.16. Though the accuracy of values estimated is not clear, the second mode damping starts to decline around q=90 kPa. But we are not sure that these estimates are reliable or not.

7 Concluding Remarks

A new flutter prediction parameter applicable to the three-mode system was proposed. The analysis and simulation using a two-dimensional wing showed that it had good properties for the flutter prediction, that is, 1) the value decreases monotonically toward zero at q_F, 2) the estimate of its value can be done accurately with a small deviation. Furthermore, the feasibility for actual flutter tests was attempted by the analysis of the data observed at wind tunnel flutter tests under the stationary and non-stationary conditions, and successful results were obtained at the case that damping method did not work.

References

[1] Zimmermann N and Weissenburger J. *Prediction of Flutter Onset Speed Based on Flight Testing at Subcritical Speeds, Journal of Aircraft*, Vol. 1, No. 4, pp 190-202, 1964.

[2] Price S and Lee B. *Evaluation and Extension of the Flutter Margin Method for Flight Flutter Prediction, Journal of Aircraft*, Vol.30, No.3, pp.395-402, 1993.

[3] Matsuzaki Y and Ando Y. *Estimation of Flutter Boundary from Random Responses due to Turbulence at Subcritical Speeds, Journal of Aircraft*, Vol.18, No.10, pp.862-868, 1981.

[4] Torii H and Matsuzaki Y. *Flutter Margin Evaluation for Discrete-Time Systems, Journal of Aircraft*, Vol. 38, No. 1, pp 42-47, 2001.

[5] Bae J et al. *Extension of Flutter Prediction Parameter for Multimode Flutter Systems, Journal of Aircraft*, Vol.42, No.1, pp.285-288, 2005.

[6] McNamara J and Friedmann P. *Flutter-Boundary Identification for Time-Domain Computational Aeroelasticity, AIAA Journal*, Vol.45, No.7, pp.1546-1555, 2007.

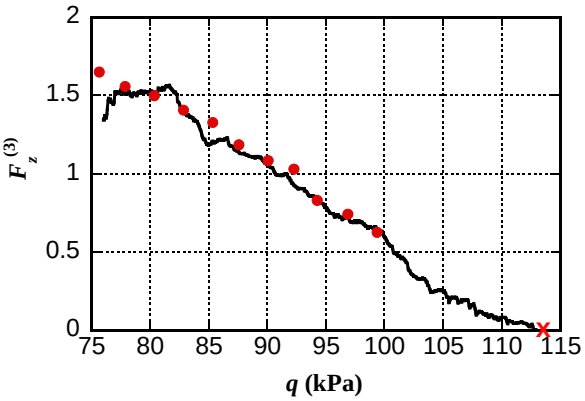

Fig.15 Real-time estimation of $F_z^{(3)}$

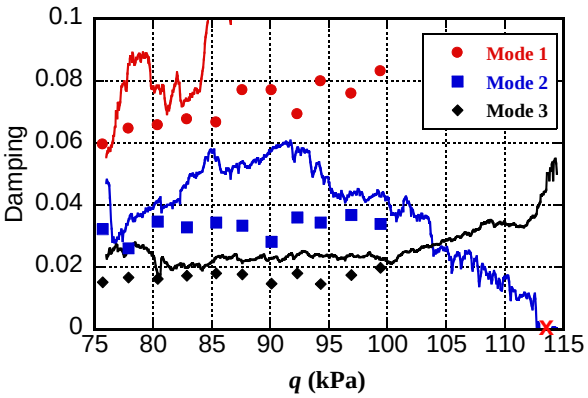

Fig.16 Real-time estimation of modal damping

Copyright Statement